JACS
JOURNAL OF THE AMERICAN CHEMICAL SOCIETY
Article
pubs.acs.org/JACS

De Novo Determination of the Crystal Structure of a Large Drug Molecule by Crystal Structure Prediction-Based Powder NMR Crystallography

Maria Baias,[†] Jean-Nicolas Dumez,[†] Per H. Svensson,[⊥,∥] Staffan Schantz,[§] Graeme M. Day,*[,‡] and Lyndon Emsley*[,†]

[†]Centre de RMN à Très Hauts Champs, CNRS/ENS-Lyon/UCB Lyon 1, Université de Lyon, 5 rue de la Doua, 69100 Villeurbanne, France

[‡]Department of Chemistry, University of Southampton, Highfield, Southampton SO17 1BJ, U.K.

[⊥]SP Process Development, Forskargatan 18, 15121 Södertälje, Sweden

[∥]Applied Physical Chemistry, Royal Institute of Technology, Teknikringen 30, 10044 Stockholm, Sweden

[§]Pharmaceutical Development, AstraZeneca R&D Mölndal, SE-431 83 Mölndal, Sweden

Supporting Information

ABSTRACT: The crystal structure of form 4 of the drug 4-[4-(2-adamantylcarbamoyl)-5-*tert*-butyl-pyrazol-1-yl]benzoic acid is determined using a protocol for NMR powder crystallography at natural isotopic abundance combining solid-state ^{1}H NMR spectroscopy, crystal structure prediction, and density functional theory chemical shift calculations. This is the first example of NMR crystal structure determination for a molecular compound of previously unknown structure, and at 422 g/mol this is the largest compound to which this method has been applied so far.

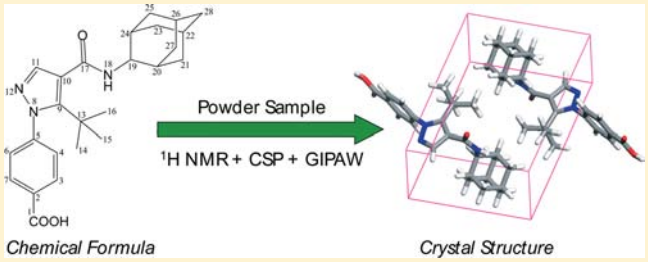

1. INTRODUCTION

The ability to determine three-dimensional molecular structures from single crystals by diffraction methods (either using X-rays or neutrons) has transformed molecular and materials science over the past 50 years, leading to today's structure-based understanding of chemistry and biochemistry. However, the problem of structure elucidation becomes much more challenging if the system under investigation exists in the form of a powder, either naturally due to the preparation of the substance, such as in the case of many pharmaceuticals, or because crystals for diffraction are unobtainable. Due to the increasing frequency with which such samples are encountered, the development of new methods for structure characterization of powder samples is an area of great current interest. It is of particular importance to the pharmaceutical industry, where structural characterization of drug polymorphs is an essential part of the overall characterization and regulation process.

Recent advances in powder crystallography have been made using both powder X-ray (or neutron) diffraction methods[1] and solid-state nuclear magnetic resonance (NMR).[2] Indeed, solid-state NMR has seen spectacular progress in the past few years, and methods have been introduced to solve crystal structures of inorganic or molecular solids.[3] For molecular solids at natural isotopic abundance, *de novo* methods have been proposed based on proton spin diffusion methods. While potentially powerful, these methods are usually experimentally very demanding. In contrast, the chemical shift is by far the easiest NMR parameter to measure, and many studies have shown that plane-wave density functional theory (DFT) calculations can now accurately reproduce measured chemical shifts in solids. This has been used to validate or refine a number of crystal structures.[4] However, the DFT structure validation approach requires a structural hypothesis as a starting point for chemical shift calculations, so it must be coupled with some means to propose sufficiently accurate putative structures.

The reliability and scope of computational methods for crystal structure prediction (CSP) have improved tremendously in recent years.[5] These methods, based on a global exploration of the lattice energy surface,[6] can provide a comprehensive prediction of the possible stable phases of a range of materials, and have been applied to the successful prediction of single[5,7] and multicomponent[5a,8] organic molecular crystals. Indeed, results of the latest blind test of structure prediction demonstrate that reasonably large pharmaceutical-like molecules are now within the scope of some of the current CSP methodologies.[5b,9]

Recently, we have shown that a protocol combining CSP, measured ^{1}H NMR chemical shifts, and DFT chemical shift calculations can accurately determine the structure of crystalline

Received: August 28, 2013
Published: October 29, 2013

   dx.doi.org/10.1021/ja4088874 | *J. Am. Chem. Soc.* 2013, 135, 17501−17507

molecular solids from powder samples. The method has so far been demonstrated successfully on four model compounds (thymol, flutamide, flufenamic acid, and cocaine)[10] with previously known structures (determined from single-crystal X-ray diffraction).

Here we use this method to determine *de novo* the crystal structure of a polymorph of a larger compound with previously unknown structure, and having as a starting point only its known chemical formula, 4-[4-(2-adamantylcarbamoyl)-5-*tert*-butyl-pyrazol-1-yl]benzoic acid (**1**, Scheme 1, also referred to as AZD8329),[11] a pharmaceutical compound with potential for the treatment of Type 2 diabetes that is an inhibitor of 11β-hydroxysteroid dehydrogenase type 1 (11β-HSD1). 11β-HSD1 is a NADPH-dependent reductase that converts cortisone to cortisol,[12] and its inhibition could reduce intracellular glucocorticoid concentrations.[13] **1** has been found to show significant polymorphism, with at least seven ansolvate/solvate forms known today. Of the major anhydrous forms 1−4, the structures of forms 1 and 4 were of particular interest since they had been chosen for development due to their suitable material properties. The former structure (form 1) had been determined by single-crystal diffraction, but the structure of form 4 remained unsolved. The two chosen forms are enantiotropically related, with form 4 found to be the more stable at ambient conditions and form 1 being the stable high-temperature crystal form. The compound has a molecular weight of 422 g/mol, and the structure of form 4 of AZD8329 is determined for the first time here.

Scheme 1. Chemical Structure of AZD8329 (1) and the Labeling Scheme Used Here

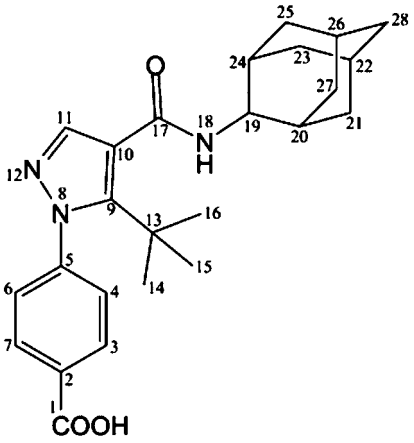

2. EXPERIMENTAL SECTION

Materials. The materials used in the current work were obtained from AstraZeneca R&D in Bangalore. Final isolation steps used for form 4 were filtration at 20−25 °C in THF/water followed by cooling crystallization in acetonitrile from 68 °C and finally drying to a powder. For form 1, AZD8329 was charged together with isopropyl and water and then dissolved in 5 N sodium hydroxide and filtered before addition of hydrochloric acid solution. Finally, the material was crystallized by cooling from 52 °C in acetone and dried under vacuum at 60 °C.

NMR Experiments. All NMR experiments were performed at a nominal temperature of 293 K with a Bruker Avance III spectrometer operating at ^{1}H and ^{13}C Larmor frequencies of 500 and 125 MHz, respectively. One-dimensional ^{1}H magic angle spinning (MAS) spectra were recorded with a 1.3 mm double-resonance probe under 60 kHz MAS using less than 10 mg of powder for each sample. One-dimensional ^{13}C cross-polarization MAS (CP-MAS) NMR spectra were recorded with 4 mm double- or triple-resonance probes at 12.5 kHz MAS using about 40 mg of sample for each sample. ^{1}H chemical shifts were referenced to the single resonance observed for protons in adamantane at 1.87 ppm with respect to the signal for neat TMS. ^{13}C chemical shifts were referenced to the CH_2 resonance observed for adamantane at 38.48 ppm with respect to the signal for neat TMS.[14]

2D refocused ^{13}C−^{13}C INADEQUATE[15] NMR spectra were recorded with a 4 mm triple-resonance probe at 12.5 kHz MAS. The SPINAL-64[16] sequence with a proton nutation frequency ν_1 of 80 kHz was used for heteronuclear decoupling. A total of 1024 increments with 256 transients each were acquired with a repetition delay of 3 s, resulting in a total experimental time of 9 days for each polymorph. The acquisition time in t_2 was 32 ms, and the ramped CP contact pulse was 3 ms. Exponential line broadening of 40 Hz was applied in both dimensions prior to the Fourier transform.

2D ^{1}H−^{13}C HETCOR spectra were recorded with a 4 mm triple-resonance CP-MAS probe at a spinning frequency of 12.5 kHz. The SPINAL-64[16] sequence with a proton nutation frequency of 100 kHz was used for heteronuclear decoupling. The eDUMBO-1_{22}[17] sequence with a nutation frequency of 100 kHz was used for proton homonuclear decoupling in the indirect dimension. The spectrum shown in the figure has a ^{1}H axis corrected for the homonuclear decoupling scaling factor of 0.54. For the HETCOR spectrum 256 scans were acquired for each of 192 increments with a repetition delay of 3 s, resulting in a total experimental time of 2 days. The ramped CP contact pulse was 3 ms. The acquisition time in t_2 was 27 ms. Exponential line broadening of 20 Hz was applied in both dimensions prior to Fourier transform. The States-TPPI procedure was used for quadrature detection in the indirect dimension for all two-dimensional experiments.

Calculations and Comparison with Experiment. Starting from the known chemical formula of **1** (Scheme 1) and without any structural hypothesis, crystal structures were predicted by exploring the lattice energy surface for the most stable local minima. The conformational diversity of AZD8329 was first assessed by calculating the torsional energy profile around all exocyclic single bonds, leading to six nontrivial degrees of freedom in the structure, and these were combined to generate an ensemble of starting conformations. *Cis*−*trans* isomerization commonly occurs in organic molecules,[18] although one of the two conformations usually has a much lower energy. For **1**, our calculations indicate that the conformations with a *trans* configuration of the amide bond are significantly more stable than conformations with the *cis* amide. Crystal structures were generated with both *cis* and *trans* conformations in case the synthesis or crystallization conditions fixed the molecule in one or the other conformation or improved intermolecular interactions could stabilize the higher energy *cis* form.

Trial crystal structures were generated independently with each of 80 starting molecular conformations in the 32 most commonly observed space groups for organic molecular crystals ($P1$, $P\bar{1}$, $P2_1$, $P2_1/c$, $P2_12_12$, $P2_12_12_1$, $Pna2_1$, $Pca2_1$, $Pbca$, $Pbcn$, $C2/c$, Cc, $C2$, Pc, $P2/c$, $C222_1$, $Fdd2$, $Iba2$, $Pccn$, $Pnma$, $P4_1$, $I\bar{4}$, $P42/n$, $I4_1/a$, $P4_12_12$, $P\bar{4}2_1c$, $P3_1$, $R3$, $R\bar{3}$, $P3_12_1$, $R3c$, $P6_1$). To generate trial crystal structures, we used a quasi-Monte Carlo method with unit cell parameters, molecular positions, and molecular orientations sampled using low-discrepancy sequences in the CrystalPredictor code.[19] These structures were further optimized (unit cell, molecular positions, and conformations) using a molecular mechanics description of the inter- and intramolecular forces, following the method outlined in ref 20 using the OFF module of the Cerius2 software package [Cerius2, version 4.6, 2001, Accelrys Inc., San Diego, CA]. The final relative energies of the lowest energy structures were calculated as a combination of a DFT calculation for the intramolecular contribution and an atom−atom model of intermolecular interactions, including an atomic multipole description of the electrostatics using the crystal modeling software DMACRYS.[21] All molecular DFT calculations were performed using the Gaussian03 software.[22]

The distribution of total energies relative to the most stable structure of all the predicted *trans* structures (in light blue) and all the

dx.doi.org/10.1021/ja4088874 | J. Am. Chem. Soc. 2013, 135, 17501−17507

predicted *cis* structures (in dark blue) is displayed in Figure 1. Only the most physically realistic structures, those within 30 kJ/mol in total

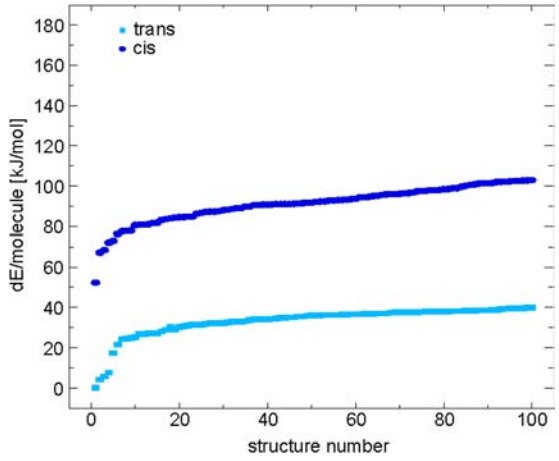

Figure 1. Predicted energy difference per molecule for all predicted structures with respect to the most stable structure as a function of structure number. The predicted structures for the *trans* conformation of the peptide bond are shown in light blue, and the predicted structures for the *cis* conformation of the peptide bond are shown in dark blue.

energy of the most stable predicted crystal structure in either the *cis* or the *trans* sets, were considered for the NMR analysis and for further DFT geometry optimizations using the CASTEP software package. As the purpose of the study was to generate an ensemble of physically reasonable structures, from which the observed forms would be selected by chemical shifts, coverage of conformational and crystal packing phase space was prioritized over the accuracy of final energies in the time scale available for the calculations. Therefore, due to the use of a small basis set for molecular energy calculations and reliance on force field methods to model crystal packing effects on the molecular geometry, the relative energies within this set of structures is not considered as an accurate indicator of their relative stabilities. In particular, the *cis*–*trans* energy difference seems to be exaggerated by the methods used during structure prediction. The total crystal energy difference between the lowest energy crystal structures of the *cis* and *trans* conformers is almost entirely due to the *cis*–*trans* intramolecular energy difference, which is reduced significantly by using a larger basis set and allowing a more complete optimization of the molecular geometry in the crystal structures (see Supporting Information (SI)). Due to the strong dependence on level of theory, we do not have an unequivocal calculated stability difference between the *cis* and *trans* structures, but we are confident that this is much smaller than the ∼50 kJ/mol energy differences indicated by the initial structure prediction calculations.

Prior to the chemical shift calculations, proton positions in each of the predicted structures were first optimized by plane-wave DFT geometry optimization with the unit cell and all heavy atom positions fixed. Chemical shieldings were then calculated for each of the proton-optimized structures. For form 1, whose crystal structure is already known, this plane-wave DFT optimization of proton positions provides a clearer identification of the correct structure from the set of predictions, as illustrated in Figure S1.

Proton position optimizations and chemical shift calculations were carried out using the DFT program CASTEP,[23] using a plane-wave basis set whose implicit translational symmetry is very well adapted to describing crystalline systems. The GIPAW method, used with ultrasoft Vanderbilt-type pseudopotentials,[24] provides an efficient method to calculate chemical shifts in crystalline solids.[25] The geometry optimizations and NMR calculations were carried out using the generalized gradient approximation (GGA) functional PBE,[26] a plane-wave energy cutoff of 600 eV, and a Monkhorst–Pack grid of *k*-points[27] corresponding to a maximum spacing of 0.05 $Å^{-1}$ in reciprocal space. These values were tested for convergence of calculated chemical shieldings on the form 1 polymorph.

For each predicted structure, the calculated chemical shielding σ_i was converted into calculated chemical shift δ_i using the relation $\delta_i = \sigma_{ref} - \sigma_i$, with the value of σ_{ref} determined by a linear regression between calculated and experimental shifts for that predicted structure.

3. RESULTS AND DISCUSSION

Here we determine the crystal structure of form 4 of **1** for which there is no previous crystal structure. Using our method, we also confirm the previously determined X-ray structure of form 1, which consists of four molecules arranged in a $P2_1/c$ monoclinic space group with a *trans* orientation of the peptide bond. A detailed description of the validation of the crystal structure of form 1 can be found in the SI.

Assignment of NMR Spectra. For both forms, carbon-13 chemical shifts were assigned with a natural abundance two-dimensional refocused $^{13}C-^{13}C$ INADEQUATE[3b] NMR spectrum which provides the connectivities between bonded carbons. We note that the assignment of the resonances of the adamantane group are ambiguous, in that we cannot *a priori* tell which branch is which, though the carbons on the different branches are not equivalent. The proton chemical shifts were then obtained from a two-dimensional $^{1}H-^{13}C$ HETCOR NMR spectrum by connection to the previously assigned carbon nuclei.

Figure 2a shows the ^{1}H MAS NMR spectrum for form 4, and Figure 2b shows the simulated stick spectra of ^{1}H chemical shifts corresponding to the four different permutations of the assignment obtained from the correlation spectra shown in Figure 3. The assigned ^{1}H and ^{13}C chemical shifts for the four possible assignments are summarized in Tables S1 and S2, respectively.

Crystal Structure Determination of Form 4. For each of the predicted structures lying within 30 kJ/mol of the structure with the lowest predicted energy, chemical shifts were computed with the GIPAW approach described above. For the set of *trans* configurations this included 20 structures, and for the *cis* configurations this involved 14 structures. For each structure, the measured and calculated shifts were then compared. All four possibilities for the assignment were evaluated, and the root-mean-square deviation (rmsd) between the calculated and measured shifts for the assignment with the lowest rmsd is retained.

Figure 4 shows the lowest rmsds for ^{1}H shifts determined in this way for form 4 of **1**. We first note that, as observed previously,[10] the agreement between calculated and experimental chemical shifts is not strongly correlated with the predicted energy (in the figure, predicted structures are ordered by ascending predicted energy). Based on the agreement between calculated and experimental chemical shifts we determine structure 21, which is the *cis* structure with the lowest predicted energy, to be the correct crystal structure for this polymorph. This is the only predicted structure that yields predicted calculated chemical shifts that are in good agreement with the data, having an rms error between calculated and experimental ^{1}H chemical shifts of 0.48 ppm. This falls within the expected errors for chemical shift calculations, which we assessed on a set of 15 organic model compounds.[10] The dashed black horizontal line in Figure 4 indicates a mean rmsd error of 0.33 ppm obtained from calculating rmsds between experimental ^{1}H shifts and the DFT calculated shifts for known

dx.doi.org/10.1021/ja4088874 | J. Am. Chem. Soc. 2013, 135, 17501–17507

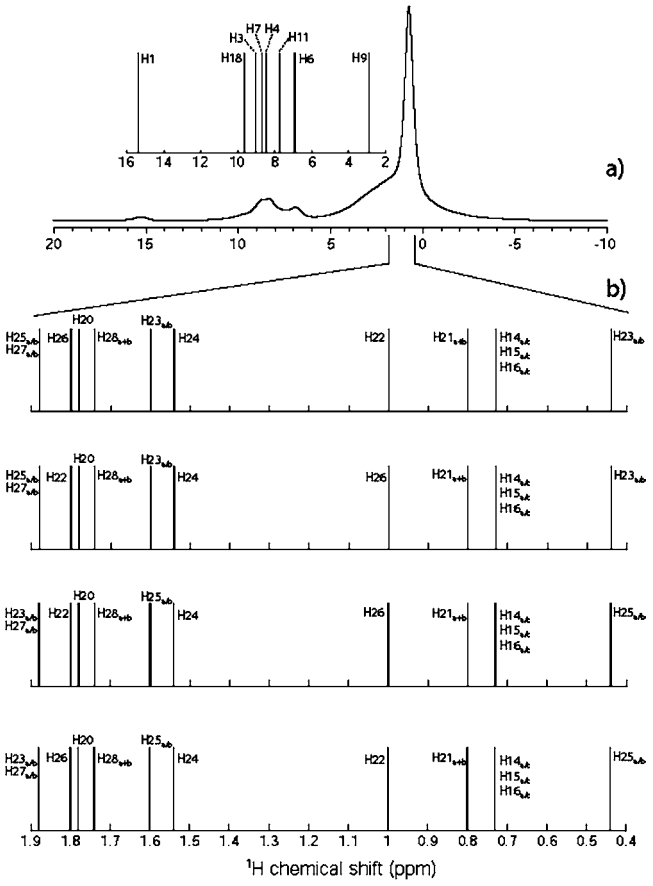

Figure 2. (a) ^{1}H 500 MHz MAS NMR spectrum of form 4 recorded at 60 kHz MAS. (b) The four different permutations of the assignment of the ^{1}H resonances based on the ^{1}H chemical shifts obtained from the spectra shown in Figure 3.

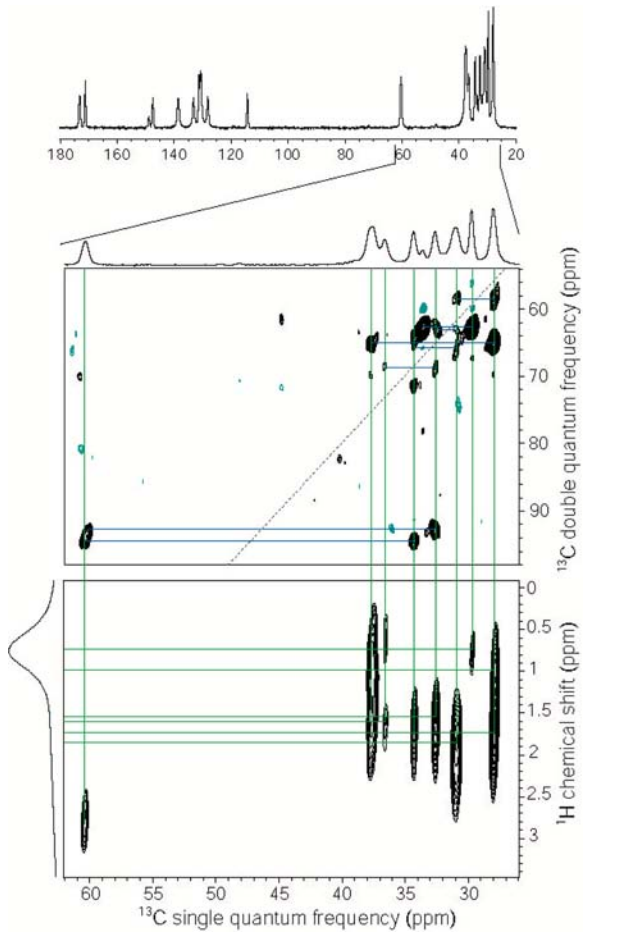

Figure 3. (Top) ^{13}C (125 MHz) CP-MAS NMR spectrum. (Middle) Expansions of the aliphatic regions of the ^{13}C−^{13}C INADEQUATE NMR spectrum. (Lower) ^{1}H−^{13}C HETCOR spectrum of form 4.

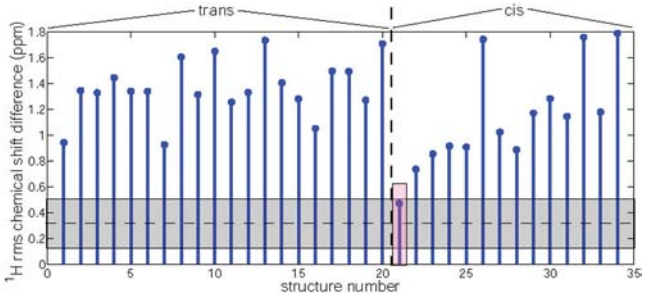

Figure 4. Comparison between experimental ^{1}H chemical shifts recorded for powdered form 4 of AZD8329 and calculated shifts for the predicted structures. Predicted structures are ordered by increasing calculated lattice energies (decreasing predicted stability). The first 20 structures correspond to the predicted most stable *trans* configurations. The remaining 14 structures correspond to *cis* configurations. The dashed horizontal black line shows the mean rmsd error as described in the text, and the horizontal gray shaded zone indicates the expected one standard deviation limits of the rmsd for good agreement in chemical shift determined from model compounds.

X-ray structures with optimized hydrogen positions, while the horizontal gray zone indicates a one standard deviation limit of the rmsd error, estimated to be ±0.16 ppm.[10] None of the other candidate structures satisfy the criteria for agreement.

This result illustrates how robust this method is, and how proton chemical shifts can be very sensitive to atomic environments. The structure determined here comprises two symmetry-equivalent molecules in a triclinic unit cell of space group $P\bar{1}$, with a unit cell volume of 1162 Å^3, and the following cell parameters: a = 10.091 Å, b = 11.399 Å, c = 11.852 Å, α = 114.87°, β = 73.29°, γ = 106.71°. The structure determined here is shown in Figure 5, and the coordinate files are given in the SI.

Finally, we note that, as seen in our previous studies,[10b] it is not possible to determine the crystal structure on the basis of the ^{13}C chemical shift rmsd (data not shown), as we have shown that ^{13}C chemical shifts do not identify the correct structure out of a set of predicted structures.

Protonation of the Carboxylic Acid Group in Form 4. Furthermore, during the course of this research we were able to determine a structure by powder X-ray diffraction (PXRD) for form 4, independently of the computational and NMR work. The heavy-atom positions of the two structures are compared in Figure S2 and agree to within an all-atom rmsd of 0.284 Å, thereby confirming the framework of the structure. However, it should be noted that the PXRD data were not sufficient to easily determine the proton positions, and in particular the protonation of the carboxylic acid group. Since the structure is not symmetric, and does not form a carboxylic acid dimer (as form 1 does), this is a significant point. In contrast, the NMR method reports the structure directly through the protons, and is therefore highly sensitive to such features.

dx.doi.org/10.1021/ja4088874 | J. Am. Chem. Soc. 2013, 135, 17501−17507

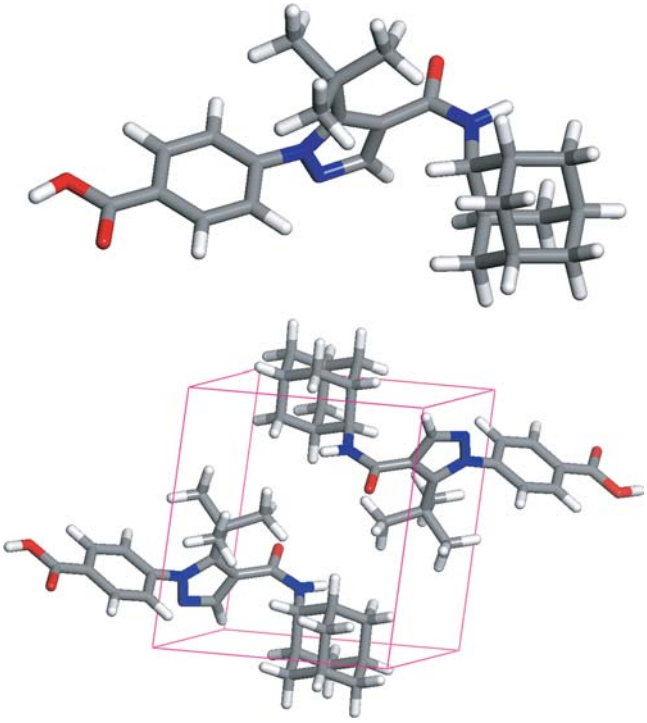

Figure 5. Structure of AZD8329 form 4 determined by powder ^{1}H NMR and computational modeling. (Top) Single molecule conformation and (Lower) the molecules as organized in the unit cell. The structure has been deposited at the Cambridge Crystallographic Data Centre under CCDC 957764.

The hydrogen-bonding network determined from the CSP/NMR structure formed by form 4 is shown in Figure 6 (bond

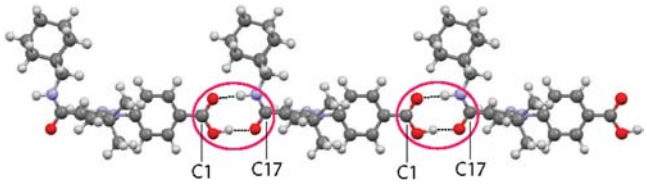

Figure 6. Illustration of the intermolecular hydrogen-bonding network in form 4 determined from the NMR structure. Note that if the carboxylic acid proton is permuted to the other oxygen, then the H-bond network cannot form.

angles and distances for the groups involved in the hydrogen bonds in the NMR-determined structure are given in Table 1). We see that the carboxylic acid group forms a double hydrogen bond to the amide group of a neighboring molecule; the OH proton donates a hydrogen bond to the amide carbonyl O atom, while the acid group carbonyl oxygen accepts a hydrogen bond from the NH group. These double hydrogen bonds

Table 1. Selected Bond Angles and Distances for the Structure of Form 4 Determined within This Study

O—H···O angle	168°
O—H bond length	1.03 Å
O···H(O) bond length	1.67 Å
N—H···O angle	165°
N—H bond length	1.04 Å
O···H(N) bond length	1.77 Å

connect translationally related molecules into hydrogen-bonded chains running along the crystallographic *c*-axis. Apart from the physical considerations that render this configuration highly probable, if we calculate chemical shifts for a structure in which the acid proton is positioned on the other oxygen atom of the carboxylic acid group, it is satisfying to find that very poor agreement with experiment is obtained. We conclude that the CSP/NMR structure contains the correct position for the acid proton.

4. CONCLUSIONS

The crystal structure of form 4 of AZD8329 (**1**) was determined by a powder NMR crystallography protocol using crystal structure prediction and DFT chemical shift calculations in combination with measured ^{1}H chemical shifts. With a molecular weight of 422 g/mol, AZD8329 is the largest molecule so far tackled by this protocol for NMR powder crystallography. Furthermore, form 4 is the first example of the *de novo* NMR crystal structure determination of a molecular solid of previously unknown structure.

■ ASSOCIATED CONTENT

Supporting Information

Full description of the CSP method and X-ray experiments, as well as the coordinate files of all the predicted structures in CIF format and the NMR-CASTEP calculation files. A description of the validation by NMR crystallography of the previously known structure of form 1. The following figures are also shown: rmsd plot comparing the ^{1}H rmsds for the CSP structures and the ^{1}H optimized structures, structure comparison between heavy atoms of form 4 determined here and the structure suggested by PXRD, experimental 1D and 2D NMR spectra of form 1, chemical shift rmsd plot for form 1, structure comparison between the form 1 determined here and the structure suggested by single-crystal XRD. We also provide a description of the PXRD data of form 4, as well as a comparison between the experimentally recorded PXRD pattern of form 4 and the one simulated for the form 4 structure determined in this study by NMR crystallography. This material is available free of charge via the Internet at http://pubs.acs.org.

■ AUTHOR INFORMATION

Corresponding Authors

g.m.day@soton.ac.uk
lyndon.emsley@ens-lyon.fr

Notes

The authors declare no competing financial interest.

■ ACKNOWLEDGMENTS

This work was supported in part by the Agence Nationale de la Recherche (ANR-2010-BLAN-0806-01). G.M.D. is supported by a Royal Society University Research Fellowship.

■ REFERENCES

(1) (a) Harris, K. D. M.; Cheung, E. Y. *Chem. Soc. Rev.* **2004**, *33*, 526−538. (b) Smith, E. D. L.; Hammond, R. B.; Jones, M. J.; Roberts, K. J.; Mitchell, J. B. O.; Price, S. L.; Harris, R. K.; Apperley, D. C.; Cherryman, J. C.; Docherty, R. *J. Phys. Chem. B* **2001**, *105*, 5818−5826. (c) Vogt, F. G.; Katrincic, L. M.; Long, S. T.; Mueller, R. L.; Carlton, R. A.; Sun, Y. T.; Johnson, M. N.; Copley, R. C. B.; Light, M. E. *J. Pharm. Sci.* **2008**, *97*, 4756−4782. (d) Dudenko, D.; Kiersnowski,

A.; Shu, J.; Pisula, W.; Sebastiani, D.; Spiess, H. W.; Hansen, M. R. *Angew. Chem., Int. Ed.* **2012**, *51*, 11068−11072.
(2) Emsley, L. Spin Diffusion for NMR Crystallography. In *Encyclopedia of NMR*; Harris, R. K., Grant, D. M., Eds.; Wiley: Chichester, 2009.
(3) (a) Lesage, A.; Auger, C.; Caldarelli, S.; Emsley, L. *J. Am. Chem. Soc.* **1997**, *119*, 7867−7868. (b) Lesage, A.; Charmont, P.; Steuernagel, S.; Emsley, L. *J. Am. Chem. Soc.* **2000**, *122*, 9739−9744. (c) Rossini, A. J.; Zagdoun, A.; Hegner, F.; Schwarzwälder, M.; Gajan, D.; Copéret, C.; Lesage, A.; Emsley, L. *J. Am. Chem. Soc.* **2012**, *134*, 16899−16908.
(4) (a) Yates, J.; Dobbins, S.; Pickard, C.; Mauri, F.; Ghi, P.; Harris, R. *Phys. Chem. Chem. Phys.* **2005**, *7*, 1402−1407. (b) Webber, A. L.; Emsley, L.; Claramunt, R. M.; Brown, S. P. *J. Phys. Chem. A* **2010**, *114*, 10435−10442. (c) Webber, A. L.; Elena, B.; Griffin, J. M.; Yates, J. R.; Pham, T. N.; Mauri, F.; Pickard, C. J.; Gil, A. M.; Stein, R.; Lesage, A.; Emsley, L.; Brown, S. P. *Phys. Chem. Chem. Phys.* **2010**, *12*, 6970. (d) Harris, R. *Analyst* **2006**, *131*, 351−373. (e) Abraham, A.; Apperley, D. C.; Gelbrich, T.; Harris, R. K.; Griesser, U. J. *Can. J. Chem.* **2011**, *89*, 770−778. (f) Harris, R. K.; Hodgkinson, P.; Zorin, V.; Dumez, J.-N.; Elena-Herrmann, B.; Emsley, L.; Salager, E.; Stein, R. S. *Magn. Reson. Chem.* **2010**, *48*, S103−S112. (g) Salager, E.; Stein, R. S.; Pickard, C. J.; Elena, B.; Emsley, L. *Phys. Chem. Chem. Phys.* **2009**, *11*, 2610−2621. (h) Webber, A. L.; Masiero, S.; Pieraccini, S.; Burey, J. C.; Tatton, A. S.; Iuga, D.; Pham, T. N.; Spada, G. P.; Brown, S. P. *J. Am. Chem. Soc.* **2011**, *133*, 19777−19795. (i) Harris, R. K.; Joyce, S. A.; Pickard, C. J.; Cadars, S.; Emsley, L. *Phys. Chem. Chem. Phys.* **2006**, *8*, 1. (j) Harris, R. K.; Cadars, S.; Emsley, L.; Yates, J. R.; Pickard, C. J.; Jetti, R. K. R.; Griesser, U. J. *Phys. Chem. Chem. Phys.* **2007**, *9*, 360. (k) Mifsud, N.; Elena, B.; Pickard, C. J.; Lesage, A.; Emsley, L. *Phys. Chem. Chem. Phys.* **2006**, *8*, 3418. (l) Sebastiani, D.; Goward, G.; Schnell, I.; Spiess, H. W. *J. Mol. Struct. (THEOCHEM)* **2003**, *625*, 283−288. (m) Brouwer, D. H.; Langendoen, K. P.; Ferrant, Q. *Can. J. Chem.* **2011**, *89*, 737−744. (n) Goward, G. R.; Sebastiani, D.; Schnell, I.; Spiess, H. W.; Kim, H.-D.; Ishida, H. *J. Am. Chem. Soc.* **2003**, *125*, 5792−5800. (o) Brown, S. P.; Schaller, T.; Seelbach, U. P.; Koziol, F.; Ochsenfeld, C.; Klarner, F. G.; Spiess, H. W. *Angew. Chem., Int. Ed.* **2001**, *40*, 717−720. (p) Ochsenfeld, C.; Brown, S. P.; Schnell, I.; Gauss, J.; Spiess, H. W. *J. Am. Chem. Soc.* **2001**, *123*, 2597−2606. (q) Heider, E. M.; Harper, J. K.; Grant, D. M. *Phys. Chem. Chem. Phys.* **2007**, *9*, 6083−6097.
(5) (a) Jones, J. T. A.; Hasell, T.; Wu, X.; Bacsa, J.; Jelfs, K. E.; Schmidtmann, M.; Chong, S. Y.; Adams, D. J.; Trewin, A.; Schiffman, F.; Cora, F.; Slater, B.; Steiner, A.; Day, G. M.; Cooper, A. I. *Nature* **2011**, *474*, 367−371. (b) Kazantsev, A. V.; Karamertzanis, P. G.; Adjiman, C. S.; Pantelides, C. C.; Price, S. L.; Galek, P. T. A.; Day, G. M.; Cruz-Cabeza, A. J. *Int. J. Pharm.* **2011**, *418*, 168−178. (c) Neumann, M. A.; Leusen, F. J. J.; Kendrick, J. *Angew. Chem., Int. Ed.* **2008**, 47. (d) Vasileiadis, M.; Kazantsev, A. V.; Karamertzanis, P. G.; Adjiman, C. S.; Pantelides, C. C. *Acta Crystallogr., Sect. B* **2012**, *68*, 677−685.
(6) Day, G. M. *Crystallogr. Rev.* **2011**, *17*, 3−52.
(7) (a) Mooij, W. T. M.; Eijck, B. P. v.; Kroon, J. *J. Am. Chem. Soc.* **2000**, *122*, 3500−3505. (b) Kendrick, J.; Stephenson, G. A.; Neumann, M. A.; Leusen, F. J. J. *Cryst. Growth Des.* **2013**, *13*, 581−589. (c) King, M. D.; Blanton, T. N.; Misture, S. T.; Korter, T. M. *Cryst. Growth Des.* **2011**, *11*, 5733−5740. (d) Adams, D. J.; Morris, K.; Chen, L.; Serpell, L. C.; Bacsa, J.; Day, G. M. *Soft Matter* **2010**, *6*, 4144−4156. (e) Bhardwaj, R. M.; Price, L. S.; Price, S. L.; Reutzel-Edens, S. M.; Miller, G. J.; Oswald, I. D. H.; Johnston, B. F.; Florence, A. J. *Cryst. Growth Des.* **2013**, *13*, 1602−1617.
(8) (a) Cruz-Cabeza, A. J.; Day, G. M.; Jones, W. *Chem. Eur. J.* **2008**, *14*, 8830−8836. (b) Eijck, B. P. v.; Kroon, J. *Acta Crystallogr. B* **2000**, *56*, 535−542. (c) Görbitz, C. H.; Dalhus, B.; Day, G. M. *Phys. Chem. Chem. Phys.* **2010**, *12*, 8466−8477. (d) Karamertzanis, P. G.; Kazantsev, A. V.; Issa, N.; Welch, G. W. A.; Adjiman, C. S.; Pantelides, C. C.; Price, S. L. *J. Chem. Theory Comput.* **2009**, *5*, 1432. (e) Leusen, F. J. J. *Cryst. Growth Des.* **2003**, *3*, 189−192. (f) Braun, D. E.; Karamertzanis, P. G.; Price, S. L. *Chem. Commun.* **2011**, *47*, 5443−5445. (g) Cruz-Cabeza, A. J.; Karki, S.; Fabian, L.; Friscic, T.; Day, G. M.; Jones, W. *Chem. Commun.* **2010**, *46*, 2224−2226.
(9) (a) Bardwell, D. A.; Adjiman, C. S.; Arnautova, Y. A.; Bartashevich, E.; Boerrigter, S. X. M.; Braun, D. E.; Cruz-Cabeza, A. J.; Day, G. M.; Valle, R. G. D.; Desiraju, G. R.; Eijck, B. P. v.; Facelli, J. C.; Ferraro, M. B.; Grillo, D.; Habgood, M.; Hofmann, D. W. M.; Hofmann, F.; Jose, K. V. J.; Karamertzanis, P. G.; Kazantsev, A. V.; Kendrick, J.; Kuleshova, L. N.; Leusen, F. J. J.; Maleev, A. V.; Misquitta, A. J.; Mohamed, S.; Needs, R. J.; Neumann, M. A.; Nikylov, D.; Orendt, A. M.; Pal, R.; Pantelides, C. C.; Pickard, C. J.; Price, L. S.; Price, S. L.; Scheraga, H. A.; Streek, J. v. d.; Thakur, T. S.; Tiwari, S.; Venuti, E.; Zhitkov, I. K. *Acta Crystallogr. B* **2011**, *67*, 535−551. (b) Santos, S. M.; Rocha, J.; Mafra, L. *Cryst. Growth Des.* **2013**, *13*, 2390−2395.
(10) (a) Salager, E.; Day, G. M.; Stein, R. S.; Pickard, C. J.; Elena, B.; Emsley, L. *J. Am. Chem. Soc.* **2010**, *132*, 2564−2566. (b) Baias, M.; Widdifield, C. M.; Dumez, J.-N.; Thompson, H. P. G.; Cooper, T. G.; Salager, E.; Bassil, S.; Stein, R. S.; Lesage, A.; Day, G. M.; Emsley, L. *Phys. Chem. Chem. Phys.* **2013**, *15*, 8069−8080.
(11) Scott, J. S.; deSchoolmeester, J.; Kilgour, E.; Mayers, R. M.; Packer, M. J.; Hargreaves, D.; Gerhardt, S.; Ogg, D. J.; Rees, A.; Selmi, N.; Stocker, A.; Swales, J. G.; Whittamore, P. R. O. *J. Med. Chem.* **2012**, *55*, 10136−10147.
(12) Edwards, C. R. W.; Benediktsson, R.; Lindsay, R. S.; Seckl, J. R. *Steroids* **1996**, *61*, 263−269.
(13) (a) Tomlinson, J. W.; Walker, E. A.; Bujalska, I. J.; Draper, N.; Lavery, G. G.; Cooper, M. S.; Hewison, M.; Stewart, P. M. *Endocrinol. Rev.* **2004**, *25*, 831−866. (b) Thieringer, R.; Hermanowski-Vosatka, A. *Exp. Rev. Cardiovasc. Ther.* **2005**, *3*, 911−924. (c) Wamil, M.; Seckl, J. R. *Drug Discovery Today* **2007**, *12*, 504−520.
(14) Morcombe, C.; Zilm, K. *J. Magn. Reson.* **2003**, *162*, 479−486.
(15) Lesage, A.; Bardet, M.; Emsley, L. *J. Am. Chem. Soc.* **1999**, *121*, 10987−10993.
(16) Fung, B.; Khitrin, A.; Ermolaev, K. *J. Magn. Reson.* **2000**, *142*, 97−101.
(17) Elena, B.; de Paepe, G.; Emsley, L. *Chem. Phys. Lett.* **2004**, *398*, 532−538.
(18) Bauer, J.; Spanton, S.; Henry, R.; Quick, J.; Dziki, W.; Porter, W.; Morris, J. *Pharm. Res.* **2001**, *18*, 859−866.
(19) Karamertzanis, P. G.; Pantelides, C. C. *J. Comput. Chem.* **2005**, *26*, 304−324.
(20) Day, G. M.; Motherwell, W. D. S.; Jones, W. *Phys. Chem. Chem. Phys.* **2007**, *9*, 1693−1704.
(21) Price, S. L.; Leslie, M.; Welch, G. W. A.; Habgood, M.; Price, L. S.; Karamertzanis, P. G.; Day, G. M. *Phys. Chem. Chem. Phys.* **2010**, *12*, 8478−8490.
(22) Frisch, M. J.; Trucks, G. W.; Schlegel, H. B.; Scuseria, G. E.; Robb, M. A.; Cheeseman, J. R.; Montgomery, J. A.; Vreven, T.; Kudin, K. N.; Burant, J. C.; Millam, J. M.; Iyengar, S. S.; Tomasi, J.; Barone, V.; Mennucci, B.; Cossi, M.; Scalmani, G.; Rega, N.; Petersson, G. A.; Nakatsuji, H.; Hada, M.; Ehara, M.; Toyota, K.; Fukuda, R.; Hasegawa, J.; Ishida, M.; Nakajima, T.; Honda, Y.; Kitao, O.; Nakai, H.; Klene, M.; Li, X.; Knox, J. E.; Hratchian, H. P.; Cross, J. B.; Bakken, V.; Adamo, C.; Jaramillo, J.; Gomperts, R.; Stratmann, R. E.; Yazyev, O.; Austin, A. J.; Cammi, R.; Pomelli, C.; Ochterski, J. W.; Ayala, P. Y.; Morokuma, K.; Voth, G. A.; Salvador, P.; Dannenberg, J. J.; Zakrzewski, V. G.; Dapprich, S.; Daniels, A. D.; Strain, M. C.; Farkas, O.; Malick, D. K.; Rabuck, A. D.; Raghavachari, K.; Foresman, J. B.; Ortiz, J. V.; Cui, Q.; Baboul, A. G.; Clifford, S.; Cioslowski, J.; Stefanov, B. B.; Liu, G.; Liashenko, A.; Piskorz, P.; Komaromi, I.; Martin, R. L.; Fox, D. J.; Keith, T.; Laham, A.; Peng, C. Y.; Nanayakkara, A.; Challacombe, M.; Gill, P. M. W.; Johnson, B.; Chen, W.; Wong, M. W.; Gonzalez, C.; Pople, J. A. *Gaussian 03*, Revision C.02; Gaussian Inc.: 2003.
(23) Clark, S. J.; Segall, M. D.; Pickard, C. J.; Hasnip, P. J.; Probert, M. I. J.; Refson, K.; Payne, M. C. *Z. Kristallogr.* **2005**, *220*, 567−570.
(24) (a) Laasonen, K.; Car, R.; Lee, C.; Vanderbilt, D. *Phys. Rev. B: Condens. Matter* **1991**, *43*, 6796−6799. (b) Vanderbilt, D. *Phys. Rev. B: Condens. Matter* **1990**, *41*, 7892−7895.

(25) Yates, J. R.; Pickard, C. J.; Mauri, F. *Phys. Rev. B* **2007**, *76*, 024401.
(26) Perdew, J.; Burke, K.; Ernzerhof, M. *Phys. Rev. Lett.* **1996**, *77*, 3865−3868.
(27) Monkhorst, H.; Pack, J. *Phys. Rev. B: Condens. Matter* **1976**, *13*, 5188−5192.